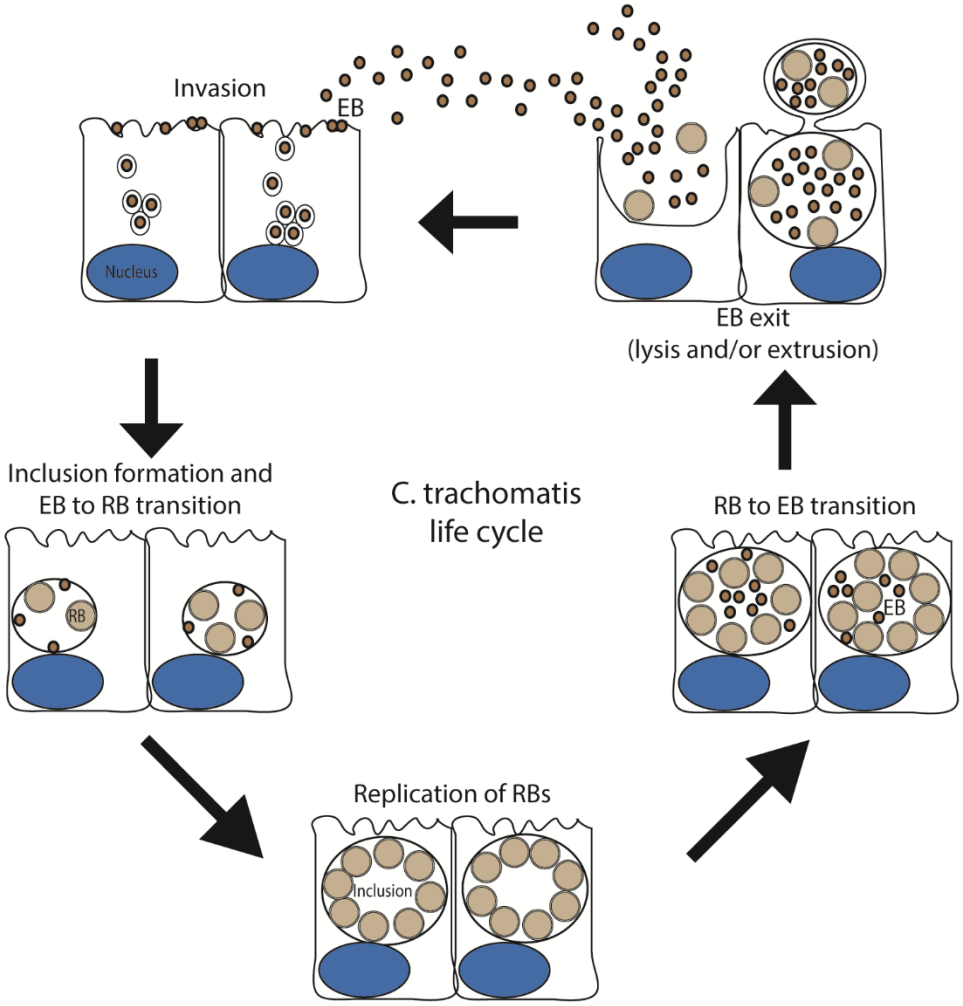

Figure S1, related to Figure 1. *Chlamydia trachomatis* life cycle.
Following internalization into cells, elementary bodies (EBs) migrate to the microtubule organizing center where they form an inclusion. Two to 6 hours post internalization EBs differentiate into reticulate bodies (RBs). By 12 hours post infection (h.p.i) RBs begin dividing by binary fission and around 24 h.p.i differentiate asynchronously back to EBs. RB's continue differentiating until lysis or release occurs approximately 48 h.p.i (Hatch 1999).

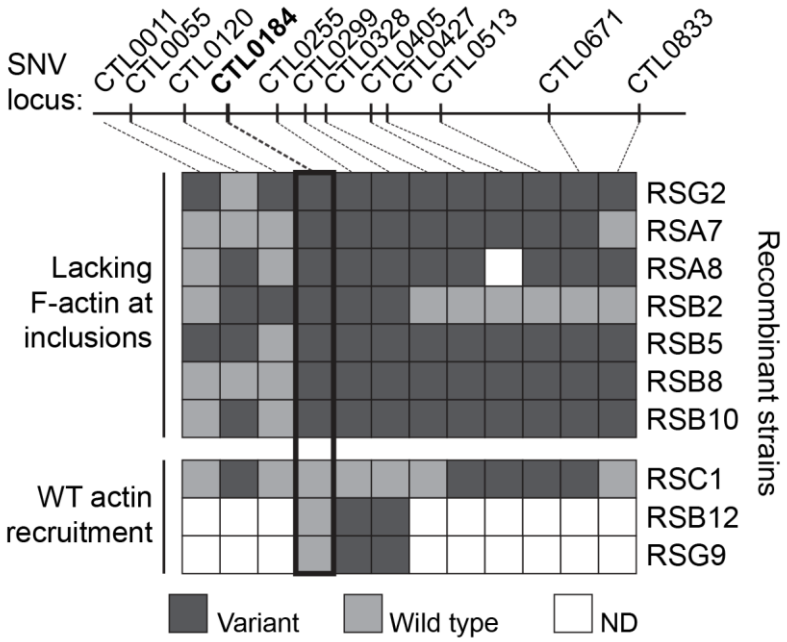

Figure S2, related to Figure 3. Loss of F-actin assembly at M407 inclusions maps to a nonsense mutation in *CTL0184.*

Mutant M407 harbors 1 non-sense SNV and 11 non-synonymous SNVs (tick marks). Co-segregation of each SNV with the absence (top) or presence (bottom) of F-actin at inclusions was assessed among recombinants generated from a co-infection between M407 (Rif^R) and a Spc^R LGV-L2 wild type strain. Each row depicts the genotype of nucleotide variants present in the parental M407 strain. Note that all recombinant progeny lacking F-actin at inclusions inherited the *CTL0184* mutant allele.

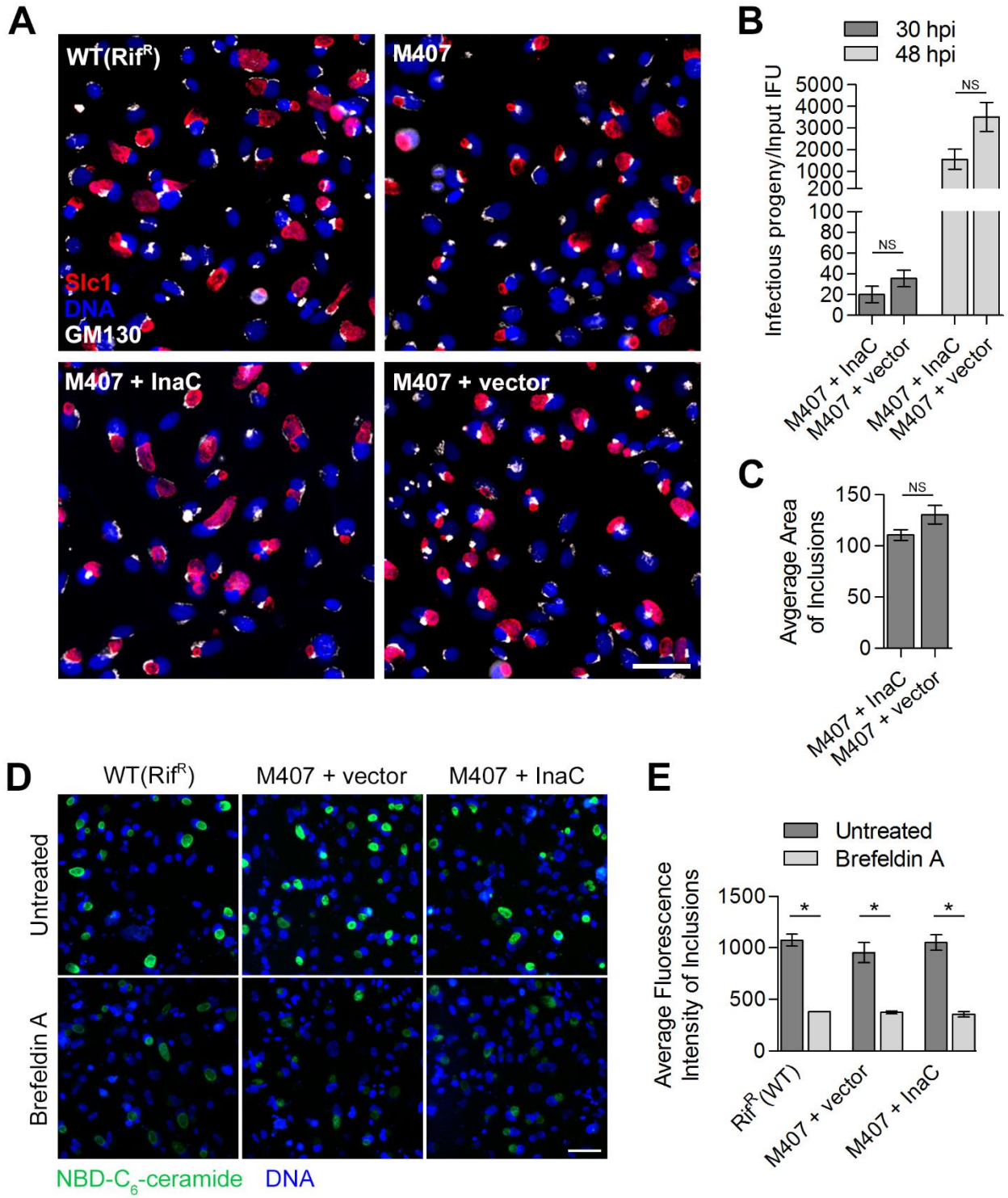

Figure S3, related to Figure 4. InaC is dispensable for bacterial growth, inclusion expansion, and sphingolipid traffic to the *C. trachomatis* inclusion.
(**A**) Golgi redistribution around the inclusion requires InaC. HeLa cells were infected with the indicated LGV-L2 strains and processed at 30 hpi for immunofluorescence using anti-GM130 (grayscale) anti-Slc1 (inclusions, red) antibodies and Hoechst (blue).

Note that while the Golgi surrounds, as subjectively assessed by GM130 distribution halfway or more around inclusions, a portion of wild type or M407 + InaC inclusions, the Golgi remains compact in cells infected with InaC-deficient strains.
(**B**) InaC expression in M407 does not enhance the strain's replication potential. The recovery of infectious progeny is not significantly different between M407 transformed with a plasmid encoding *inaC* or an empty vector. At 30 and 48 hpi, HeLa cells infected with the indicated strains at an MOI of 0.6 were harvested and the resulting infectious progeny were enumerated and normalized to the number of input bacteria.
(**C**) InaC expression in M407 does not alter inclusion size. At 24 hpi, cells infected as in (A) were processed for immunofluorescence with anti-Slc1 antibodies to define inclusions. The average area of at least 100 inclusions was measured.
(**D and E**) Accumulation of fluorescent sphingolipids within inclusions is not significantly different between wild type or M407 transformed with an empty vector or a plasmid encoding *inaC*. HeLa cells were infected at an MOI of 3 with the indicated strains and at 23 hpi labeled with NBD-C_6-ceramide (green) followed by a 6 hour back-exchange, stained with Hoechst (blue), imaged (C), and assessed for the mean fluorescence intensity (D) of at least 90 inclusions in each triplicate. As a control, cells were incubated with 3 µg/mL Brefeldin A for 30 minutes prior to labeling and throughout the back-exchange.
Mean ± SEM for three independent experiments, each done in triplicate, is shown. * indicates $P < 0.05$ and NS indicates $P > 0.05$ by one-way ANOVA and Newman-Keuls *post hoc* (A), Student's t test (B), or two-way ANOVA with Bonferroni *post hoc* (D). Scale bars represent 50µm.

Table S5, related to Figure 4: Proteins that co-IP with GFP-InaC as identified by LC-MS/MS

Identified Proteins	Protein Name	Accession Number[1]	Total Spectrum Count[2]		Exclusive Unique Peptide Count	
			GFP	GFP-InaC	GFP	GFP-InaC
Hypothetical protein CT813 [*Chlamydia trachomatis* D/UW-3/CX]	CT813/ InaC	GI:15605547	0	101	0	20
14-3-3 protein epsilon	1433E	P62258	0	68	0	21
14-3-3 protein zeta/delta	1433Z	P63104	0	58	0	12
14-3-3 protein beta/alpha	1433B	P31946	0	47	0	8
14-3-3 protein gamma	1433G	P61981	0	41	0	10
ADP-ribosylation factor 1	ARF1	P84077	0	38	0	7
14-3-3 protein theta	1433T	P27348	0	36	0	9
14-3-3 protein eta	1433F	Q04917	0	32	0	13
Transcription intermediary factor 1-beta	TIF1B	Q13263	0	30	0	19
ADP-ribosylation factor 4	ARF4	P18085	0	29	0	6
ADP-ribosylation factor 5	ARF5	P84085	0	27	0	3
Probable ATP-dependent RNA helicase DDX49	DDX49	Q9Y6V7	0	18	0	11
Transcription elongation factor SPT5	SPT5H	O00267	0	11	0	10
Acidic leucine-rich nuclear phosphoprotein 32 family member A	AN32A	P39687	0	11	0	7
Nucleophosmin	NPM	P06748	0	5	0	3
ATPase family AAA domain-containing protein 3B	ATD3B	Q5T9A4	0	5	0	2
ATPase family AAA domain-containing protein 3C	ATD3C	Q5T2N8	0	5	0	0
Protein SET	SET	Q01105	0	4	0	4
Acidic leucine-rich nuclear phosphoprotein 32 family member B	AN32B	Q92688	0	4	0	2
ATPase family AAA domain-containing protein 3A	ATD3A	Q9NVI7	0	4	0	0

[1] UniProtKB/Swiss-Prot Accession Number.

[2] Analysis limited to proteins with more than two Total Spectrum Counts.

SUPPLEMENTAL EXPERIMENTAL PROCEDURES

Cell lines, *Chlamydia* strains, growth conditions, and antibodies

Vero cells (ATCC CCL-81) and HeLa cells were grown in high glucose DMEM supplemented with L-glutamine, sodium pyruvate (Gibco, Life Technologies) and 10% FBS (Mediatech, CellGro), at 37 ºC in a 5% CO_2 humidified incubator. Rifampin resistant (Rif^R) and spectinomycin resistant (Spc^R) *C. trachomatis* LGV biovar L2 434/Bu strains have been previously described ((Nguyen and Valdivia., 2012), Supplementary table S3 in (Snavely and Kokes et al., 2014)). All *Chlamydia* strains were maintained as frozen stocks in SPG buffer (0.25 M sucrose, 10 mM sodium phosphate, 5 nM glutamic acid). LGV L2 infections were performed with EBs from crude cell lysates of infected cells, synchronized by centrifugation (2,500 x g for 30 minutes at 10 ºC) onto Vero and HeLa cell monolayers, and incubated for indicated times. EB titers were determined by infecting Vero cell monolayers seeded in a 96 well plate. At 30 hpi cells were fixed and stained with anti-Slc1 antibodies. The number of Inclusion forming units (IFUs) were determined using a Cellomics ArrayScan automated fluorescence imaging system (Thermo Scientific). Antibody and plasmid sources: rabbit anti-*Chlamydia* MOMP (Kenneth Fields, University of Kentucky), mouse anti-CT813 (Guangming Zhong, University of Texas Health and Science Center), rabbit anti-GAPDH (Abcam), rabbit anti-Slc1 (Chen et al., 2014), rabbit anti-IncG (Ted Hackstadt, NIAID Rocky Mountain Laboratories), rabbit anti-14-3-3ε (Cell Signalling), rabbit anti-14-3-3β (Santa Cruz), mouse anti-GM130 (BD Biosciences), mouse anti-GFP (Clontech), EGFP-ARF vectors (Marci Scidmore), and *C. trachomatis* Serovar D Gateway ORFeome (Roan et al., 2006).

Generation of a *C. trachomatis* LGV-L2 mutant library

Chemical mutagenesis. Vero cells infected with Rif^R LGV-L2 were exposed to 20 mg/mL ethyl methyl sulfonate (EMS) and 3 mg/mL N-ethyl-N-nitrosourea (ENU) as previously described (Nguyen and Valdivia., 2012). At 72 hpi, mutagenized EBs were harvested by hypotonic lysis of infected cells, IFUs tittered, and lysates stored in SPG at -80 ºC.

Isolation of small plaque-forming mutant strains. Following mutagenesis, monolayers of Vero cells seeded in 6-well plates were infected with 100 IFUs/well from independent pools of mutagenized EBs. At 2 hpi, infected cells were overlaid with DMEM/agarose (0.5 % SeaKem LE agarose (Lonza), 1X DMEM, 10% FBS, 25 µg/mL gentamycin (Gibco), 1X nonessential amino acids (Gibco), 200 ng/mL cycloheximide (Sigma-Aldrich)) and supplemented with 200 ng/mL rifampin (Sigma-Aldrich). Plaques were allowed to form for 7 to 10 days and bacteria from small plaques were harvested by coring plaques with a pipette tip and infecting Vero cell monolayers in 96 well plates in DMEM supplemented with 5% FBS and 200 ng/mL cycloheximide. Infections were carried out until large inclusions were visible (48-120 hpi) and EBs were harvested as described above. A second expansion step was performed in Vero cell monolayers seeded in 24 well plates and EBs harvested as described above. Cell lysates containing EBs were arrayed into 96 well plates to establish an ordered collection of mutant strains.

Preparation and sequencing of genomic libraries from the *C. trachomatis* LGV-L2 mutant library

Enrichment of C. trachomatis DNA for sequencing. Vero cell monolayers in T25 flasks were grown in DMEM supplemented with 5% BSA and 200 ng/mL cycloheximide and infected with 100 µl of crude infected cell lysates derived from each strain in the mutant collection (see above). Infected cells were incubated until large inclusions were observed (48-120 hpi). Mutants exhibiting severely attenuated growth rates were expanded several times until robust infections were observed. At time of harvest, EBs were concentrated from cell lysates by centrifugation (21,000 x g, 15 minutes, 4 ºC), and resuspended in DNAse I reaction buffer (NEB Labs). Residual host DNA was digested with 8 Units of DNAse I (NEB) for 1 hour at 37 ºC and EBs washed with 500 µl PBS, pelleted by centrifugation, and resuspended in 180 µl of ATL buffer (Qiagen). Total DNA was isolated with a Qiagen DNeasy Blood and Tissue Kit (Qiagen) according to the manufacturer instructions.

Whole genome sequencing. 150 ng of total DNA isolated from each of 20 individual strains were pooled with 150 ng of DNA from a mutant strain that had been previously sequenced. One µg of pooled genomic DNA was sheared by ultrasound with an Adaptive Focused Acoustics S220 instrument (Covaris). Sequencing libraries were prepared and barcoded with a TrueSeq DNA sample preparation kit (Illumina Inc.) according to the manufacturers instructions. Five barcoded libraries (21 DNA genomes per library) were sequenced per lane of a HiSeq2000 sequencing platform (Illumina Inc.).

Detection of single nucleotide variants from pooled sequencing data

All raw sequencing data has been deposited in the NCBI Sequence Read Archive (Kodama et al., 2012) and can be accessed through accession number SRP049629. Bioinformatic analysis of mutant pool sequences was conducted using a combination of existing software and new tools developed for this analysis. The software developed specifically for this project can be downloaded from https://bitbucket.org/granek/ct_snvome. This repository contains everything necessary to reproduce the analysis and figures, once required software is installed, and raw sequence data is downloaded from the NCBI Sequence Read Archive.

Sequence read mapping. Sequencing data generated in the Illumina platform was binned by barcode sequence, and 50 mer single end reads aligned to the *C. trachomatis* L2/434/Bu reference sequence (GenBank NC_010287) with BWA (BWA-bactrack algorithm; version 0.7.5a-r405) (Li and Durbin., 2009). SAM files from BWA were converted to BAM, sorted, and indexed using SAMtools (version 0.1.18) (Li et al., 2009).

Single nucleotide variant calling. Putative SNVs were identified from pooled samples using SNVer (Wei et al., 2011). Because sequencing pools were comprised of 21 mutant genomes, SNVer parameters for Number of Haploid Genomes and Number of Samples were set to 21. For all other SNVer parameters, defaults were used and SNVer run with the following modifications: Reads were not quality filtered prior to using

SNVer. Duplicate removal was omitted since optical or PCR duplicates were not observed in our data. Omitting this step increased SNV detection sensitivity. SNVer run time was reduced by using software developed for running multiple instances of SNVer in an embarrassingly parallel manner (see repository address above for all custom software). Bonferroni correction was omitted and custom software using Statsmodels Python library was used for applying a Benjamini-Hochberg procedure to raw p-value outputs from SNVer for multiple comparison corrections. The false discovery rate for all SNVs was controlled at 5%.

Single nucleotide variant effect on gene product function. Predicted amino acid changes resulting from non-synonymous SNVs were classified as having a neutral or non-neutral effect on gene product function using SNAP (Bromberg and Rost., 2007).

Central metabolism and DNA repair pathway analysis
C. trachomatis LGV L2 central metabolism and DNA repair pathways were inferred from genome annotations using KEGG (Kyoto Encyclopedia of Genes and Genomes) pathway tools provided by PATRIC (Pathosystems Resource Integration Center; www.patricbrc.org. (Wattam et al., 2014))

Forward genetics screen for F-actin recruitment defective mutants
HeLa cells were grown to 50% confluency in 96-well plates and infected with 10 µl of crude cell lysates derived from each mutant in the library. As controls, cells were infected with varying amounts of density gradient purified wild type EBs at MOIs ranging from 0.1-100. At 30 hpi, cells were fixed and stained with rabbit anti-Slc1 antibodies followed by Alexa488 conjugated Goat anti Rabbit IgG (Life Technologies), Rhodamine-Phalloidin (Life Technologies), and Hoechst. Cells were imaged with Cellomics HTC Arrayscan (Thermo Scientific) and images viewed with Cellomics vHCS: View Software v1.6 (Thermo Scientific) to visually assess F-actin at the periphery of inclusions. The MOIs of infections with mutant strains ranged from 0.1 to 50.

Identification of InaC (CTL0184)
M407 whole genome sequencing. Chlamydia DNA was isolated from M407 as described above and sequenced in a MiSeq sequencing platform (Illumina Inc.). Read mapping and SNV calling was performed by reference-based assembly to the *C. trachomatis* L2/434/Bu (GenBank NC_010287) genome with Geneious Pro v6 software (Biomatters).

Generation of recombinants. Vero cells were co-infected with M407 (Rif^R) and a Spc^R strain at an MOI ratio of 3:3. At 44 hpi, progeny were harvested by hypotonic lysis and Rif^R/Spc^R doubly resistant recombinant strains isolated by plaque assay as described in (Nguyen and Valdivia., 2012). All recombinants isolated were assessed for F-actin assembly at inclusions.

Genotyping. Seven recombinants lacking F-actin assembly at inclusions and one recombinant displaying wild-type actin recruitment were genotyped for all M407

encoded SNVs through TILLING as previously described (Colbert et al., 2001; Kari et al., 2011), and by Sanger sequencing for the SNV in CTL0299.

Complementation of M407 with wild type InaC

Vector construction and transformation. The CTL0184 ORF (*inaC*) and 250 b. p of upstream sequence were amplified from *C.t* LGV L2 genomic DNA by PCR and inserted into the shuttle vector p2TK2-SW2 (Agaisse and Derré., 2013). M407 was transformed with either empty vector or the vector containing wild type *CTL0184* as previously described (Wang et al., 2011) to create the M407 + vector and M407 + InaC strains. Transformants were plaque purified under Penicillin G selection (1 U/mL).

Immunoblot. HeLa cells grown to 50% confluency were infected with the indicated strains at an MOI of 1 and at 30 hpi cell lysates prepared in 1% SDS buffer (1% SDS, 150 mM NaCl, 50 mM Tris–HCl, pH 7.5). Equal amounts of lysates were resolved by SDS-PAGE followed by immunoblot analysis with anti-CT813 (anti-InaC), anti-MOMP, and anti-GAPDH antibodies using a LI-COR (Odyssey) infrared imaging system.

Visual and quantitative analysis of F-actin assembly at inclusions

High-resolution imaging. HeLa cells grown on glass coverslips were infected with indicated *C. trachomatis* strains at an MOI of five. At 30 hpi, cells were fixed and stained with mouse anti-CT813 (anti-InaC) antibodies, rabbit anti-IncG, Alexa conjugated secondary antibodies (Life Technologies), Rhodamine-Phalloidin (Life Technologies), and Hoechst, and mounted onto glass slides with Slow Fade Gold (Invitrogen). Images were captured on an Axio Observer Z1 (Zeiss) inverted widefield fluorescence microscope with a 63X objective (Zeiss). Images were minimally processed with Image J (NIH) and Photoshop CS6 (Adobe).

Visual quantification. HeLa cells grown in 96-well plates were infected with indicated strains at an MOI of five. At 30 hpi, cells were fixed and stained as above with rabbit anti-Slc1 antibodies, Alexa488 conjugated Goat anti Rabbit IgG (Life Technologies), Rhodamine-Phalloidin (Life Technologies), and Hoechst. Cells were imaged with a Cellomics HTC Arrayscan (Thermo Scientific) and a 20x objective and images viewed with Cellomics vHCS: View Software v1.6 (Thermo Scientific) to quantify number of inclusions surrounded by F-actin for at least 60 inclusions per well. Images were analyzed with a custom-designed algorithm in Cellomics Scan Software v5.6 (Thermo Scientific) to assess average intensity of F-actin. All images were background subtracted with a 3D surface-fitting model. Inclusions were defined by anti-Slc1 staining, and 2 µm-wide ring-shaped regions were further defined by expanding out from 1 µm within the inclusion object edge. Average intensity of Rhodamine-Phalloidin fluorescence (F-actin) was measured in these regions as a mean value of all objects in a well. Background intensities were measured by defining similar ring-shaped objects around Hoechst-positive nuclei in uninfected wells, and subtracted from the average intensities of F-actin around inclusions in each experiment. At least 350 inclusions or nuclei were analyzed per well.

Statistics. Three technical triplicate wells were combined in each of three independent experiments. Within each experiment, values were normalized to values observed in

wild-type inclusions. Statistically significant differences were assessed by a one-way ANOVA followed by Newman-Keuls Multiple Comparison *post-hoc* analysis with a p-value < 0.05 considered significant. Graphs were prepared with Prism (GraphPad Software) and Photoshop (Adobe).

Identification of host proteins that interact with InaC

Vector construction. To create a plasmid for mammalian transient expression of a full-length CT813 tagged at the N-terminus with cycle 3 GFP, a Gateway entry clone containing the *C. trachomatis* Serovar D ORF CT813 from a *C. trachomatis* Gateway ORFeome library (Roan et al., 2006) was used as a donor for Gateway transfer into the destination vector pDEST53. The NEB Q5 Site-Directed Mutagenesis Kit was used to insert a stop codon at the end of the CT813 ORF.

Immunoprecipitation. HEK 293T cells grown to 50% confluency in 10 cm dishes coated with poly-L-Lysine (Sigma-Aldrich) were transfected with either a GFP-only vector (pDEST53) or a GFP-InaC plasmid using jetPRIME (Polyplus transfection) with a fresh media exchange after 4 hr. At 24 hr post transfection, cells were chilled and scraped in lysis buffer (25 mM Tris-HCl [pH 8.0], 150 mM NaCl, 1 mM EDTA, and 0.5% NP-40) supplemented with a broad protease inhibitor cocktail (Roche Diagnostics) and a broad phosphatase inhibitor (Pierce). After mechanical lysis by vigorous pipetting three times over 30 min and high speed centrifugation to remove insoluble debris, GFP-Trap (ChromoTek) resin was added and incubated overnight at 4°C. After washing thoroughly with lysis buffer, bound resin was analyzed by LC-MS/MS at the Duke Proteomics Core facility to identify proteins, or bound proteins were eluted in 0.2 M glycine [pH 2.5] and resolved by SDS PAGE and subjected to immunoblot analysis as described above.

Assessing ARF and 14-3-3 recruitment to inclusions

HeLa cells grown on glass coverslips were infected with indicated *C. trachomatis* strains at an MOI of five and transfected with plasmids encoding several EGFP-ARF fusion proteins with jetPRIME (Polyplus transfections). At 30 hpi, cells were fixed and stained with rabbit anti-14-3-3β or -ε and Hoeschst. Images were captured on an Axio Observer Z1 (Zeiss) inverted widefield fluorescence microscope with a 63X objective (Zeiss). Images were minimally processed with Image J (NIH) and Photoshop CS6 (Adobe). 14-3-3 micrographs were acquired at the same exposures across all samples. A Gaussian de-blur algorithm was applied uniformly to EGFP-ARF micrographs to reduce background from out of focus signal.

Visual and quantitative analysis of Golgi redistribution around inclusions

High-resolution imaging. HeLa cells grown on glass coverslips were infected with indicated *C. trachomatis* strains at an MOI of five. At 30 hpi, cells were fixed and stained with mouse anti-GM130 antibodies (BD Biosciences), rabbit anti-IncG, Alexa conjugated secondary antibodies (Life Technologies), and Hoechst. Images were captured on an Axio Observer Z1 (Zeiss) inverted widefield fluorescence microscope with a 63X objective (Zeiss). Images were minimally processed with Image J (NIH) and Photoshop CS6 (Adobe).

Visual quantification. HeLa cells grown in 96-well plates were infected with indicated strains at an MOI of five. At 30 hpi, cells were fixed and stained with rabbit anti-Slc1 antibodies to define inclusions, mouse anti-GM130 antibodies (BD Biosciences) to define the Golgi, Alexa conjugated secondary antibodies (Life Technologies), and Hoechst. F-actin was depolymerized with a 30 min treatment of 500 nM Latrunculin B (Life Technologies) prior to fixation, as indicated. Samples were imaged with a Cellomics HTC Arrayscan (Thermo Scientific) and a 20x objective and images viewed with Cellomics vHCS: View Software v1.6 (Thermo Scientific) and inclusions were scored as having "Golgi distributed around the inclusion" based on the subjective appearance of Golgi (defined by GM130) localized at least half-way around the inclusion (defined by Slc1). At least 50 inclusions were scored in each well.

Statistics. Three technical triplicate wells were combined in each of three independent experiments. Values are expressed as a percent. Statistically significant differences were assessed by Student's t test or a one-way ANOVA followed by Newman-Keuls Multiple Comparison *post-hoc* analysis with a p-value < 0.05 considered significant. Graphs were prepared with Prism (GraphPad Software) and Photoshop CS6 (Adobe).

Inclusion forming units (IFU) and inclusion size analysis

Confluent monolayers of HeLa cells in 96-well plates were infected with various *Chlamydia* strains at an MOI of 0.6. At 24 hpi samples were fixed and inclusions were detected by immunostaining with anti-Slc1 antibodies. Bacteria in infected cells were harvested at 30 and 48 hpi by hypotonic lysis as previously described (Nguyen and Valdivia., 2012) in duplicate. Serial dilutions of the cell lysates were used to infect a new monolayer of confluent HeLa cells and inclusions were detected by immunostaining with anti-Slc1 antibodies at 24 hpi. Cells were imaged with a Cellomics HTC Arrayscan (Thermo Scientific) and a 20x objective and images were analyzed with a custom-designed algorithm in Cellomics Scan Software v5.6 (Thermo Scientific) to analyze the total count, or IFUs, and the average area of inclusions. The total number of IFUs obtained at 30h and 48h (output) was divided by the number of input IFU to derive number of infectious progeny per input IFU. The average area reported was assessed only from input samples, which were infected uniformly at an MOI of 0.6 and are expressed as arbitrary units.

Statistics. Three technical triplicate wells were combined in each of three independent experiments. Statistically significant differences were assessed by Student's t test or a one-way ANOVA followed by Newman-Keuls Multiple Comparison *post-hoc* analysis with a p-value < 0.05 considered significant. Graphs were prepared with Prism (GraphPad Software) and Photoshop CS6 (Adobe).

Visual and quantitative analysis of sphingolipid trafficking to inclusions
We adapted a published protocol (Moore., 2012). HeLa cells grown to 50% confluency in 96-well plates were infected with the indicated LGV-L2 strains at an MOI of 3. At 23 hpi, plates were chilled to 12°C for 15 min and rinsed with cold Hanks balanced salt solution (HBSS) prior to incubation with pre-chilled 5µM NBD-C_6-ceramide (Life Technologies) in DMEM supplemented with 0.034% defatted BSA (Sigma) at 12°C for 30 min. Cells were rinsed twice with 37°C HBSS and incubated for 6 hr with DMEM supplemented with 0.7% defatted BSA for back-exchange at 37°C. Prior to imaging, cells were incubated with 2 µg/mL Hoescht in HBSS at 37°C for 10 min. Live cells were imaged with a Cellomics HTC Arrayscan (Thermo Scientific) and a 20x objective and images were analyzed with a custom-designed algorithm in Cellomics Scan Software v5.6 (Thermo Scientific) to analyze the average intensity of objects defined by an intensity threshold in the NBD-detecting channel (inclusions). As a control, cells were incubated with 3 µg/mL Brefeldin A (Sigma-Aldrich) for 30 minutes prior to labeling and throughout the back-exchange and processed identically. Images were minimally processed with Cellomics vHCS: View Software v1.6 (Thermo Scientific) and Photoshop CS6 (Adobe).

Statistics. Three technical triplicate wells were combined in each of three independent experiments. Statistically significant differences were assessed by two-way ANOVA with Bonferroni *post hoc* analysis with a p-value < 0.05 considered significant. Graphs were prepared with Prism (GraphPad Software) and Photoshop CS6 (Adobe).

REFERENCES
Agaisse, H., and Derré, I. (2013). A *C. trachomatis* cloning vector and the generation of *C. trachomatis* strains expressing fluorescent proteins under the control of a *C. trachomatis* promoter. PloS One *8*, e57090.

Bromberg, Y., and Rost, B. (2007). SNAP: predict effect of non-synonymous polymorphisms on function. Nucleic Acids Res. *35*, 3823-3835.

Colbert, T., Till, B.J., Tompa, R., Reynolds, S., Steine, M.N., Yeung, A.T., McCallum, C.M., Comai, L., and Henikoff, S. (2001). High-throughput screening for induced point mutations. Plant Physiol. *126*, 480-484.

Kari, L., Goheen, M.M., Randall, L.B., Taylor, L.D., Carlson, J.H., Whitmire, W.M., Virok, D., Rajaram, K., Endresz, V., McClarty, G., et al. (2011). Generation of targeted *Chlamydia trachomatis* null mutants. Proc. Natl. Acad. Sci. U S A *108*, 7189-7193.

Kodama, Y., Shumway, M., and Leinonen, R. (2012). The Sequence Read Archive: explosive growth of sequencing data. Nucleic Acids Res. *40*, D54-56.

Li, H., and Durbin, R. (2009). Fast and accurate short read alignment with Burrows-Wheeler transform. Bioinformatics *25*, 1754-1760.

Li, H., Handsaker, B., Wysoker, A., Fennell, T., Ruan, J., Homer, N., Marth, G., Abecasis, G., and Durbin, R. (2009). The Sequence Alignment/Map format and SAMtools. Bioinformatics *25*, 2078-2079.

Moore, E.R. (2012). Sphingolipid trafficking and purification in *Chlamydia trachomatis*-infected cells. Curr. Protoc. Microbiol. Chapter 11, Unit 11A.12.

Nguyen, B.D., and Valdivia, R.H. (2012). Virulence determinants in the obligate intracellular pathogen *Chlamydia trachomatis* revealed by forward genetic approaches. Proc. Natl. Acad. Sci. U S A *109*, 1263-1268.

Roan, N.R., Gierahn, T.M., Higgins, D.E., and Starnbach, M.N. (2006). Monitoring the T cell response to genital tract infection. Proc. Natl. Acad. Sci. U S A *103*, 12069-12074.

Snavely, E.A., Kokes, M., Dunn, J.D., Saka, H.A., Nguyen, B.D., Bastidas, R.J., McCafferty, D.G., and Valdivia, R.H. (2014). Reassessing the role of the secreted protease CPAF in *Chlamydia trachomatis* infection through genetic approaches. Pathog. Dis. *71*. 336-351.

Wang, Y., Kahane, S., Cutcliffe, L.T., Skilton, R.J., Lambden, P.R., and Clarke, I.N. (2011). Development of a transformation system for *Chlamydia trachomatis*: restoration of glycogen biosynthesis by acquisition of a plasmid shuttle vector. PLoS Pathog. *7*, e1002258.

Wattam, A.R., Abraham, D., Dalay, O., Disz, T.L., Driscoll, T., Gabbard, J.L., Gillespie, J.J., Gough, R., Hix, D., Kenyon, R., et al. (2014). PATRIC, the bacterial bioinformatics database and analysis resource. Nucleic Acids Res. *42*, 581-591.

Wei, Z., Wang, W., Hu, P., Lyon, G.J., and Hakonarson, H. (2011). SNVer: a statistical tool for variant calling in analysis of pooled or individual next-generation sequencing data. Nucleic Acids Res. *39*, 1-13.